Divergent roles of growth factors in the GnRH regulation of puberty in mice

Sara A. DiVall,[1] Tameeka R. Williams,[1] Sarah E. Carver,[1] Linda Koch,[2] Jens C. Brüning,[2,3] C. Ronald Kahn,[4] Fredric Wondisford,[1] Sally Radovick,[1] and Andrew Wolfe[1]

[1]Department of Pediatrics, Johns Hopkins University, Baltimore, Maryland, USA. [2]Department of Mouse Genetics and Metabolism, Institute for Genetics, University of Cologne, Cologne, Germany. [3]Department of Internal Medicine, University Hospital of Cologne and Max Planck Institute for the Biology of Aging, Cologne, Germany. [4]Joslin Diabetes Center, Harvard Medical School, Boston, Massachusetts, USA.

Pubertal onset, initiated by pulsatile gonadotropin-releasing hormone (GnRH), only occurs in a favorable, anabolic hormonal milieu. Anabolic factors that may signal nutritional status to the hypothalamus include the growth factors insulin and IGF-1. It is unclear which hypothalamic neuronal subpopulation these factors affect to ultimately regulate GnRH neuron function in puberty and reproduction. We examined the direct role of the GnRH neuron in growth factor regulation of reproduction using the Cre/lox system. Mice with the IR or IGF-1R deleted specifically in GnRH neurons were generated. Male and female mice with the IR deleted in GnRH neurons displayed normal pubertal timing and fertility, but male and female mice with the IGF-1R deleted in GnRH neurons experienced delayed pubertal development with normal fertility. With IGF-1 administration, puberty was advanced in control females, but not in females with the IGF-1R deleted in GnRH neurons, in control males, or in knockout males. These mice exhibited developmental differences in GnRH neuronal morphology but normal number and distribution of neurons. These studies define the role of IGF-1R signaling in the coordination of somatic development with reproductive maturation and provide insight into the mechanisms regulating pubertal timing in anabolic states.

Introduction

At pubertal onset, the hypothalamic gonadotropin-releasing hormone (GnRH) pulse generator becomes activated to trigger the hormonal cascade necessary for sexual maturation. It has been estimated that 50%–80% of the variance in timing of pubertal onset in humans is due to genetic factors, based upon calculations of heritability in large population studies (1). Thus, the remaining 20%–50% of variance is due to environmental and metabolic factors that modulate the reemergence of GnRH pulses. Pubertal onset in humans (2) and rodents (3) is associated with attainment of a particular body mass, and disease states associated with a disruption in the normal timing of puberty, including malnutrition, chronic inflammatory states, thyroid disease, and growth hormone deficiency, are also associated with metabolic disturbances (4), suggesting that a catabolic hormonal milieu suppresses GnRH activation at puberty, or conversely, that an anabolic hormonal milieu is necessary for GnRH activation at puberty.

Anabolic hormones that are candidates to influence GnRH activation at puberty include the growth factors insulin and IGF-1. A role for insulin in the neuroendocrine regulation of puberty and reproduction was suggested by the infertility of female neuron-specific insulin receptor–knockout (NIRKO) mice. These mice had low luteinizing hormone (LH) levels that increased in response to GnRH, suggesting dysfunction at the hypothalamic level (5). IGF-1, produced in response to growth hormone, is crucial to mammalian growth and increases at the time of puberty. Individuals with extremely low IGF-1, such as those with Laron syndrome, experience delayed puberty (6), suggesting that there is orchestration between the somatotropic and reproductive axes at the time of puberty. IGF-1 has been shown to modulate pubertal timing in rodents. Prepubertal rats receiving intracerebroventricular IGF-1 experienced an earlier pubertal onset, as indicated by vaginal opening, than rats given saline (7). In agreement with this finding, male rats given intracerebroventricular IGF-1 antibody experienced puberty, as indicated by serum testosterone level and testicular weight, significantly later than rats given vehicle (8). Female mice with deletion of the growth hormone receptor experience delayed puberty, as indicated by vaginal opening, that is advanced by IGF-1 administration (9). Male mice with deletion of the growth hormone receptor also experience delayed puberty (10). These data suggest that IGF-1 modulates GnRH neuron function to affect the timing of puberty.

The hypothalamus contains subpopulations of specialized neurons that sense peripheral signals to control energy balance and reproductive function. GnRH neurons contain both insulin receptors (IRs) and IGF-1 receptors (IGF-1Rs) (11–13). In vitro stimulation of GnRH neurons with insulin increases GnRH expression and release (11, 14–16). IGF-1 stimulation also increases GnRH expression (17, 18) and release (19) in vitro. We sought to determine whether direct action of insulin and IGF-1 on the GnRH neuron plays a role in regulation of puberty and reproduction in vivo. To accomplish this, we used the Cre/lox system to generate GnRH-specific IR– (GnRH-IRKO) and IGF-1R–knockout (GnRH-IGFRKO) mice. The GnRH-IRKO mice exhibited normal puberty and fertility; however, GnRH-IGFRKO mice of both sexes experienced delayed puberty, with a sexual dimorphism in pubertal timing in response to IGF-1 administration. Morphological differences in GnRH neurons during development may account for these findings, as prepubertal GnRH-IGFRKO mice exhibited differences in GnRH neuron dendritic morphology, while adult GnRH-IGFRKO mice had GnRH neuron morphology similar to that of control mice.

Results

Generation of the GnRH-IRKO mouse. Mice with IR specifically excised in neurons have hypothalamic hypogonadism, implicating signaling via

Conflict of interest: The authors have declared that no conflict of interest exists.
Citation for this article: *J Clin Invest.* 2010;120(8):2900–2909. doi:10.1172/JCI41069.

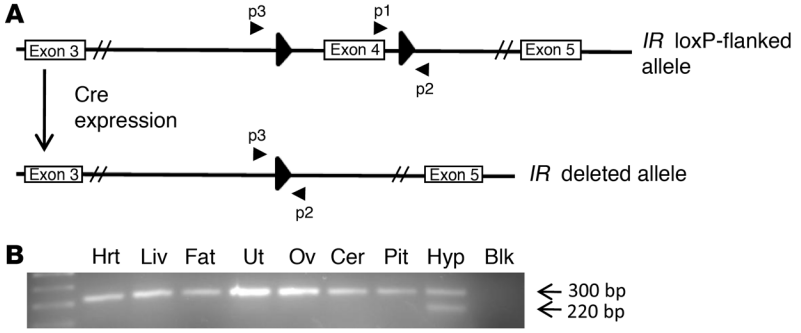

Figure 1
Generation of the GnRH-IRKO mouse. (**A**) The *IR* gene with loxP sites (large arrows) flanking exon 4 before (top panel) and after (bottom panel) recombination by Cre. Primers used for genotyping and detection of the loxP flanked or truncated *IR* gene are labeled p1, p2, and p3. (**B**) PCR of DNA was performed using primers indicated in **A**. The loxP flanked allele is indicated by the 320-bp band, while the excised *IR* gene is indicated by the 220-bp band. Hrt, heart; Liv, liver; Ut, uterus; Ov, ovary; Cer, cerebellum; Pit, pituitary; Hyp, hypothalamus; Blk, blank.

the IR as a mechanism for the nutritional regulation of reproduction (5). To generate mice with the IR specifically deleted in GnRH neurons, $IR^{fl/fl}$ mice (20) were crossed with mice expressing Cre recombinase under control of the GnRH promoter (GnRH-Cre). The GnRH-Cre transgenic mice have the Cre recombinase gene downstream from 3,446 bp of the mouse GnRH promoter and express Cre specifically in the GnRH neuron (21). The $IR^{fl/fl}$ mice were designed with loxP sites flanking exon 4; excision of exon 4 in the presence of Cre recombinase resulted in a frameshift mutation and produced a premature stop codon (Figure 1A). Matings were designed to generate the GnRH-IRKO ($Cre^{+}IR^{fl/fl}$) mice and control littermates ($Cre^{-}IR^{fl/fl}$ or $Cre^{+}IR^{fl/WT}$). To demonstrate that the *IR* gene was specifically excised in GnRH neurons, PCR of DNA was performed using primers flanking exon 4 of the *IR* gene. As shown in Figure 1B, the smaller amplicon, indicating excision of exon 4, was only found in hypothalamic tissue, not in other brain or peripheral tissue of a $Cre^{+}IR^{fl/fl}$ mouse.

Puberty and fertility are normal in GnRH-IRKO mice. To assess the reproductive phenotype of the GnRH-IRKO mice, we assessed multiple parameters. In females, vaginal opening is estradiol dependent and is indicative of the activation of the hypothalamic-pituitary-gonadal axis at puberty (22). The GnRH-IRKO mice experienced vaginal opening on the same postnatal day as control littermates (Figure 2A). The day of first estrus implies the establishment of the hormonal cyclicity necessary for female reproduction (22). Control and GnRH-IRKO mice experienced their first estrus on similar postnatal days (Figure 2A). Balanopreputial separation is testosterone dependent (23) and thus is an indicator of activation of the reproductive axis in males. Control and GnRH-IRKO mice experienced balanopreputial separation at similar ages (Figure 2A). The longitudinal change in anogenital distance (AGD) has been correlated with androgen exposure (24) and was also assessed in male mice. AGD was also not significantly different between

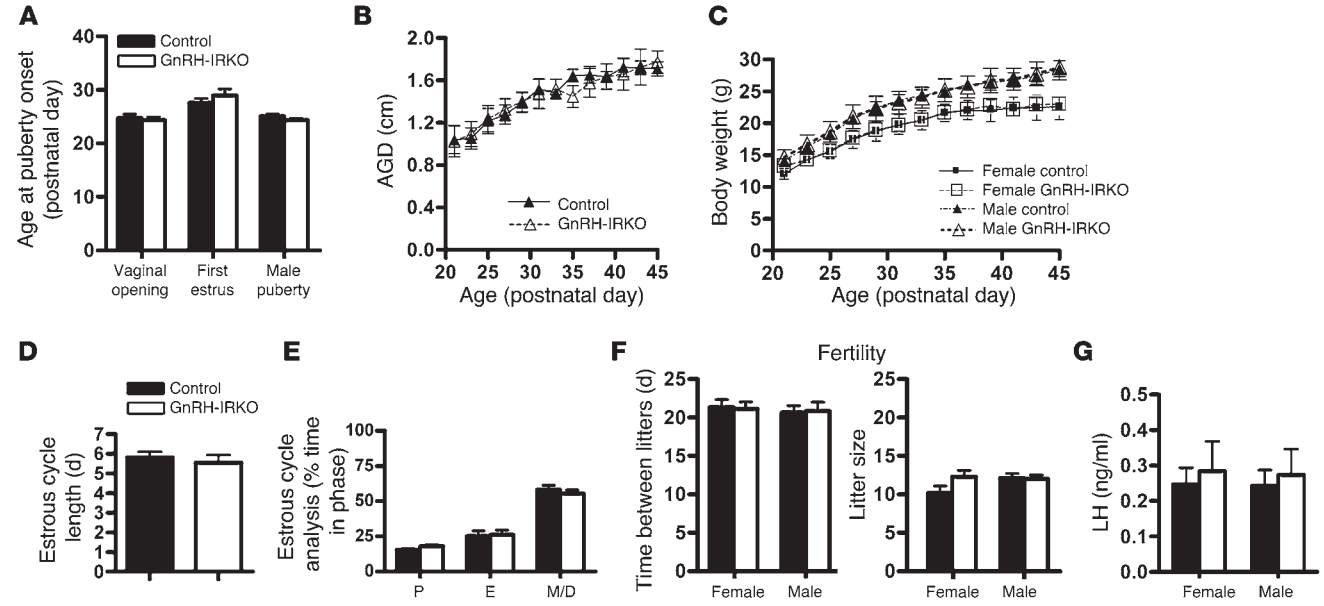

Figure 2
GnRH-IRKO mice have normal onset of puberty and reproductive function. (**A**) Pubertal evaluation included the time of vaginal opening and first estrus in control (n = 8) and GnRH-IRKO (n = 8) females and balanopreputial separation in control (n = 6) and GnRH-IRKO (n = 6) males. (**B**) AGD, which is testosterone dependent, was also assessed in males of pubertal age (n = 4 each group). (**C**) Body weight of pubertal animals (n = 5 each group). Vaginal cytology for at least 14 consecutive days was performed in 4 female mice of each genotype to evaluate estrous cycling. (**D**) Estrous cycle length. (**E**) Time in each estrous cycle phase. P, proestrus; E, estrus; M/D, metestrus/diestrus. (**F**) To assess fertility, we determined the time to birth after introduction with a male and the number of pups per litter. (**G**) Serum LH was determined in 5 adult mice of each sex and genotype. Values are mean ± SEM.

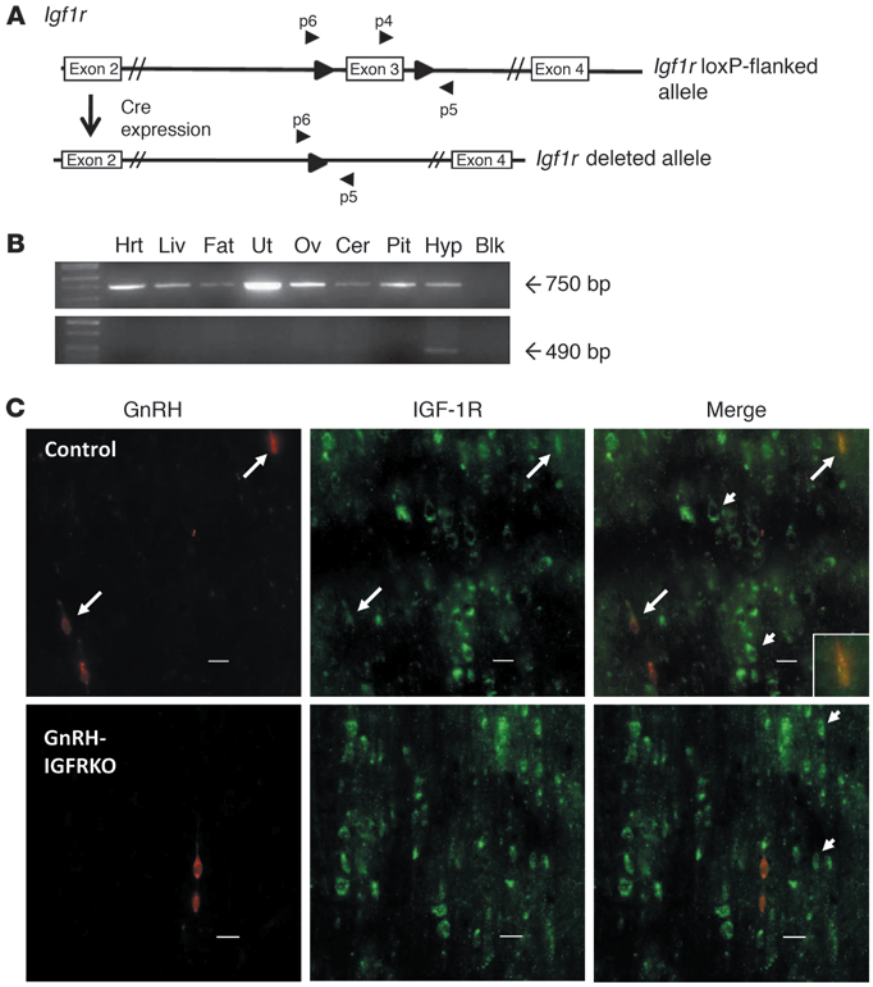

Figure 3
Generation of the GnRH-IGFRKO mouse. (**A**) The *Igf1r* gene with exon 3 flanked by loxP sites (large arrows) before (top panel) and after (bottom panel) Cre recombination. Primers used for detection of the truncated *Igf1r* gene are labeled p4, p5, and p6. (**B**) PCR analysis of genomic DNA isolated from tissues of a GnRH-IGFRKO mouse. The floxed *Igf1r* gene is indicated by the 750-bp band, and the excised *Igf1r* gene is indicated by the 490-bp band. (**C**) Sections (40 μm) of hypothalami from control littermates or GnRH-IGFRKO mice were incubated with anti-GnRH and anti–IGF-1R antibody with secondary antibodies conjugated to a fluorophore emitting red (GnRH) or green (IGFR) wavelengths. Long arrows indicate neurons that stain for GnRH and IGF-1R. Short arrows indicate neurons that stain for IGF-1R only. Scale bars: 20 μm.

control and GnRH-IRKO mice (Figure 2B). Furthermore, body weight also did not differ between GnRH-IRKO and control littermates (Figure 2C). In adults, estrous cycle length (Figure 2D) and staging (Figure 2E) did not differ between control and GnRH-IRKO mice. Male and female fertility, as measured by time to birth from mating and litter size, also did not differ (Figure 2F). Finally, serum LH did not differ between control and GnRH-IRKO female or male mice (Figure 2G).

Generation of the GnRH-IGFRKO mouse. To generate mice with the IGF-1R specifically deleted in GnRH neurons (GnRH-IGFRKO mice), Cre/lox technology was similarly used. The GnRH-Cre mice were crossed with the IGF-1R floxed mice that are described elsewhere (25, 26). The $Igf1r^{fl/fl}$ mice were designed with loxP sites flanking exon 3 such that in the presence of Cre recombinase, exon 3 would be excised (Figure 3A). Matings were designed to generate the GnRH-IGFRKO mice ($Cre^{+}Igf1r^{fl/fl}$) or control littermates ($Cre^{-}Igf1r^{fl/fl}$ or $Cre^{+}Igf1r^{fl/WT}$). To demonstrate that the *Igf1r* gene was specifically deleted in GnRH neurons, a number of techniques were used. After DNA was isolated from multiple tissues of a $Cre^{+}Igf1r^{fl/fl}$ mouse, PCR was performed using primers designed to detect the intact or incomplete *Igf1r* gene, in which exon 3 is excised. Primers spanning exon 3 detected a 750-bp band representing the intact gene. Figure 3B depicts the 750-bp band in tissues of the GnRH-IGFRKO animal including the heart, liver, fat, muscle, uterus, ovaries, cerebellum, pituitary, and hypothalamus. To detect the presence of the excised gene, primers outside the 5′ loxP site and the 3′ loxP site were used. The 490-bp knockout band was present only in the hypothalamus of the GnRH-IGFRKO mouse (Figure 3B). Other tissues of the same animal did not contain the knockout band. Thus, the *Igf1r* gene was intact in all tissues from the GnRH-IGFRKO mouse, with the hypothalamus also containing the knockout gene. To examine for the presence of IGF-1R in GnRH neurons, we performed double label immunofluorochemistry using antibodies specific for GnRH or IGF-1R (Figure 3C). Colocalization of GnRH and IGF-1R was noted in 52% of the GnRH neurons (data not shown) in $Cre^{-}Igf1r^{fl/fl}$ or $Cre^{+}Igf1r^{fl/WT}$ mice. A similar percentage of colocalization was noted by Daftary and Gore in wild-type animals (13). The area shown is the rostral preoptic area, where the greatest percentage of colocalization was noted. As expected, IGF-1R staining was also noted in surrounding cells that did not contain GnRH (Figure 3C). In GnRH-IGFRKO mice, less than 4% of neurons that stained for GnRH also stained for IGF-1R, and IGF-1R staining was also detected in surrounding cells of the rostral preoptic area (Figure 3C).

Female GnRH-IGFRKO mice experience delayed puberty. Both intracerebroventricular and peripherally administered IGF-1 have been demonstrated to advance puberty in rodents, implicating a role for IGF-1 signaling within the hypothalamus in the normal timing of

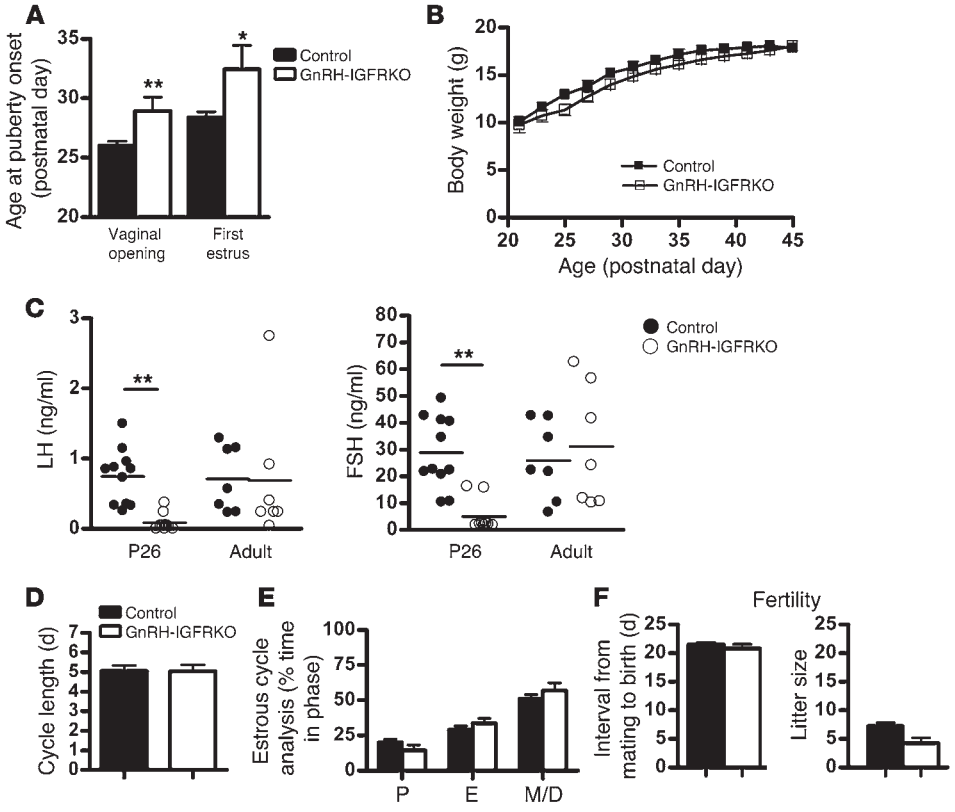

Figure 4
Female GnRH-IGFRKO mice have delayed puberty but normal adult reproductive function. (**A**) The time of vaginal opening and first estrus in littermate controls (n = 12) and GnRH-IGFRKO (n = 12) mice. (**B**) Body weight development in female mice (n = 10 each genotype). (**C**) Serum LH and FSH levels in P26 (n = 10 each genotype) and adult mice (n = 7 each genotype). Vaginal cytology for at least 14 days was performed in 6 mice of each genotype to evaluate estrous cycling in adult females. (**D**) Estrous cycle length. (**E**) Time in each estrous cycle phase. (**F**) To assess fertility, we determined the time to birth after introduction with a male and the number of pups per litter. Values are mean ± SEM. *P < 0.05, **P < 0.01.

puberty. To determine whether IGF-1 signaling specifically within the GnRH neuron plays a role in the timing of mouse puberty, we determined day of vaginal opening and day of first estrus in GnRH-IGFRKO mice and control female littermates, similar to experiments performed in GnRH-IRKO mice. The GnRH-IGFRKO females experienced vaginal opening approximately 3 days later than control littermates (P29 ± 1.1 vs. P26 ± 0.3, P < 0.01; Figure 4A). The age of first estrus was also significantly delayed in GnRH-IGFRKO animals (P32.5 ± 2.0 vs. P28.5 ± 0.5, P < 0.05; Figure 4A). Puberty in rodents is dependent upon weight (3), so the peripubertal weight of GnRH-IGFRKO and control littermates was assessed. The weight of GnRH-IGFRKO and control mice was not significantly different (Figure 4B). LH and follicle-stimulating hormone (FSH) levels were determined on P26, the day that control animals had entered puberty but the GnRH-IGFRKO animals had not. The control females had higher serum LH at P26 than GnRH-IGFRKO mice (0.74 ± 0.12 ng/ml vs. 0.08 ± 0.04 ng/ml, P < 0.01; Figure 4C), consistent with the significant delay in pubertal onset. In contrast the LH was similar in adult control and GnRH-IGFRKO females. The serum FSH was also significantly different between animals at P26 (control, 28.8 ± 4.0 ng/ml vs. GnRH-IGFRKO, 5.1 ± 1.8 ng/ml, P < 0.01) but not significantly different in adulthood. Insulin levels in fasted adult control littermates were not significantly different from those in fasted GnRH-IGFRKO mice (40.5 ± 25 vs. 28.5 ± 6.5 ng/ml). The GnRH-IGFRKO mice had estrous cycle length (Figure 4D) and percent time spent in each phase of the cycle (Figure 4E) similar to those of control mice. Finally, fertility did not differ significantly between control and GnRH-IGFRKO females (Figure 4F).

Male GnRH-IGFRKO mice experience delayed puberty. In males, the day of preputial separation of the glans penis was determined, as was the longitudinal change in AGD and testicular weight. Preputial separation occurred approximately 3 days later in GnRH-IGFRKO males than in control littermates (P29 ± 0.4 vs. P26 ± 0.3, P < 0.001; Figure 5A). AGD was not significantly shorter in GnRH-IGFRKO mice at weaning (P21) but was significantly shorter in GnRH-IGFRKO mice at P25 (0.79 ± 0.09 cm in GnRH-IGFRKO mice vs. 1.05 ± 0.05 cm in control mice; P < 0.001), shortly before the control littermates entered puberty at P26 (Figure 5B). AGD continued to be significantly shorter in GnRH-IGFRKO males than in control littermates until P33. Testicular weights were also determined at different ages, as testicular weight increases at the time of puberty in response to LH stimulation. At P24 the testicular weights were not different between control littermates and GnRH-IGFRKO mice (Figure 5C). On P26, the testicular weights of control mice were significantly greater than those of GnRH-IGFRKO mice (104 ± 2.9 mg vs. 75 ± 3.6 mg; P < 0.05). This difference persisted until P30, when the testicular weights of GnRH-IGFRKO mice were no longer significantly different from those of control mice. The testicular weights of adult (P60) GnRH-IGFRKO males were not significantly different from those of control males. The peripubertal body weights of the GnRH-IGFRKO and control mice were not significantly different (Figure 5D). The control males had higher serum LH on P26 than GnRH-IGFRKO males (0.95 ± 0.18 ng/ml vs. 0.30 ± 0.09 ng/ml, P < 0.05; Figure 5E). FSH at that age was significantly higher in control males (227 ± 27 ng/ml vs. 38 ± 29 ng/ml, P < 0.01). LH and FSH in adult control males were not significantly different from those in GnRH-IGFRKO mice. Insulin levels were not significantly different in fasted control adult littermates compared with fasted GnRH-IGFRKO adults (201 ± 121 ng/ml vs. 152 ± 35 ng/ml). Fertility was not different between control and GnRH-IGFRKO males (Figure 5F).

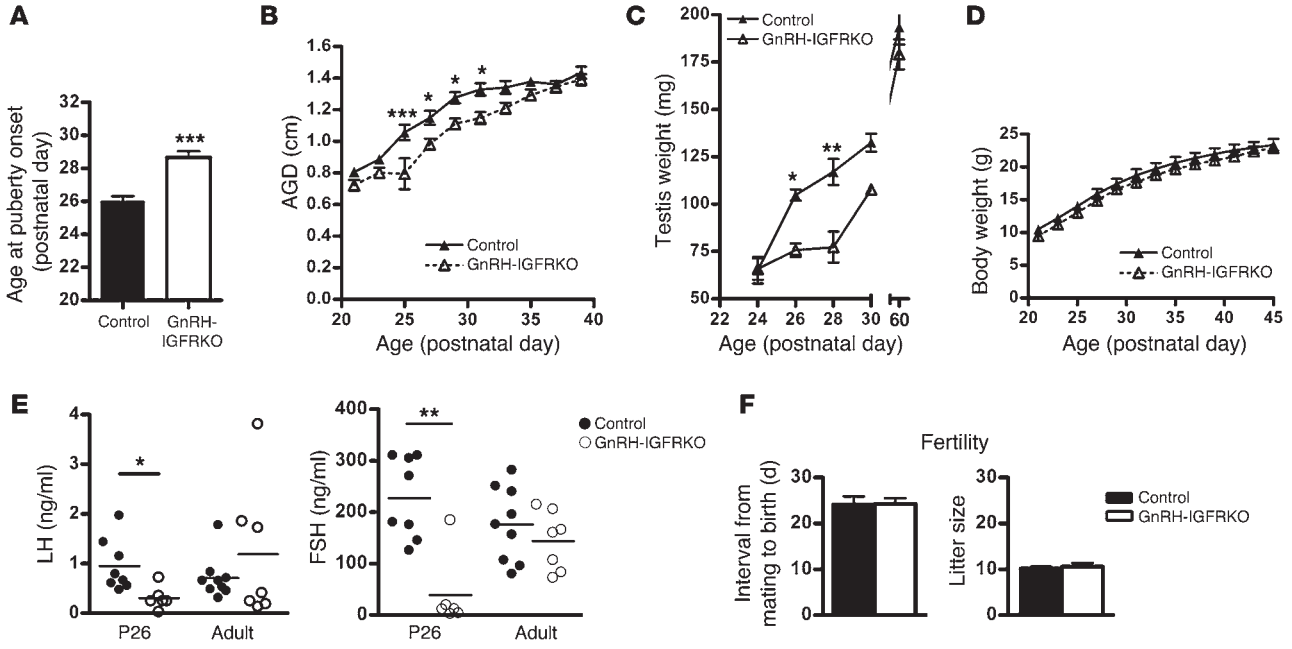

Figure 5
Male GnRH-IGFRKO mice have delayed puberty but normal adult reproductive function. (**A**) The age of preputial separation was assessed in littermate controls ($n = 12$) and GnRH-IGFRKO ($n = 12$) males. (**B**) AGD development ($n = 9$ each genotype). (**C**) Testicular weight development ($n = 5$ each postnatal day and genotype). (**D**) Body weight development in male mice ($n = 10$ each genotype). (**E**) Serum LH and FSH levels in P26 ($n = 8$ control, $n = 6$ GnRH-IGFRKO) and adult male mice ($n = 9$ control, $n = 7$ GnRH-IGFRKO). (**F**) Fertility assessment of control and GnRH-IGFRKO mice. Values are mean ± SEM. $^*P < 0.05$, $^{**}P < 0.01$, $^{***}P < 0.001$.

Peripheral IGF-1 treatment differentially advances puberty. To determine whether IGF-1R signaling plays an active or permissive role in the timing of puberty, we administered IGF-1 to prepubertal mice. On P16, ten days before pubertal onset in control mice, 20 μg/g IGF-1 was administered subcutaneously twice daily, and vaginal opening or preputial separation was assessed. Control female mice administered vehicle experienced vaginal opening on approximately P26 (±0.3), while control female mice administered IGF-1 experienced vaginal opening significantly earlier, on approximately P23 (±0.3) ($P < 0.05$; Figure 6A). Female GnRH-IGFRKO mice administered vehicle had vaginal opening on P29 (±0.6). IGF-1 treatment did not result in a statistically significant age advancement of vaginal opening (P27 ± 1.5) in the GnRH-IGFRKO mice.

The same treatment paradigm was performed in males. Control male mice that received IGF-1 experienced preputial separation on approximately P25, not significantly different from mice treated with vehicle (P25 ± 0.4; Figure 6B). A similar absence of response to IGF-1 was observed in GnRH-IGFRKO male mice (vehicle on P29 ± 0.6; IGF-1 on P29 ± 0.5). Thus, IGF-1 administration did not advance puberty in male mice.

GnRH neuron development is abnormal in GnRH-IGFRKO mice. IGF-1R signaling in neurons has been demonstrated to be important for neuronal progenitor proliferation, neurite outgrowth, and synaptogenesis (27). GnRH neurons migrate from the olfactory placode to the hypothalamus early in gestation, and the factors necessary for migration have yet to be elucidated. It is unknown whether IGF-1 signaling in GnRH neurons plays a role in GnRH neuronal migration or development. To investigate the role of IGF-1 signaling in GnRH neuronal migration, we determined the number and distribution of GnRH neurons in GnRH-IGFRKO and control littermates. Immunohistochemistry using an antibody specific to GnRH was performed on adult mice. Figure 7A indicates the number of neurons counted in successive regions of the hypothalamus in control and GnRH-IGFRKO mice. There was no difference noted

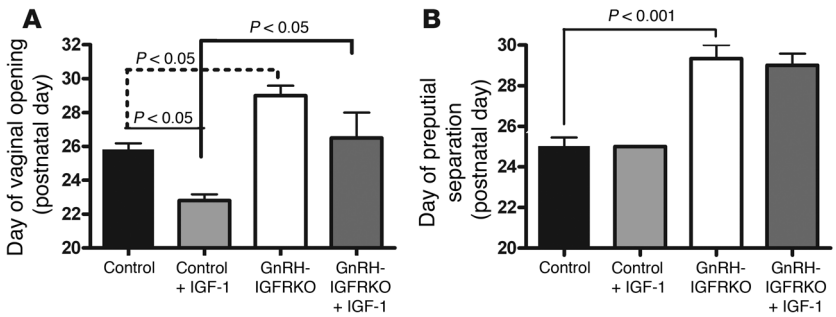

Figure 6
IGF-1 affects pubertal timing. (**A**) Prepubertal female control littermates were administered vehicle ($n = 5$) or IGF-1 ($n = 5$), as were female GnRH-IGFRKO mice ($n = 4$ vehicle, $n = 4$ IGF-1), subcutaneously from P16 until day of vaginal opening. (**B**) Prepubertal male control littermates were administered vehicle ($n = 5$) or IGF-1 ($n = 5$), as were male GnRH-IGFRKO mice ($n = 3$ vehicle, $n = 3$ IGF-1), subcutaneously from P16 until full balanopreputial separation. Values are mean ± SEM.

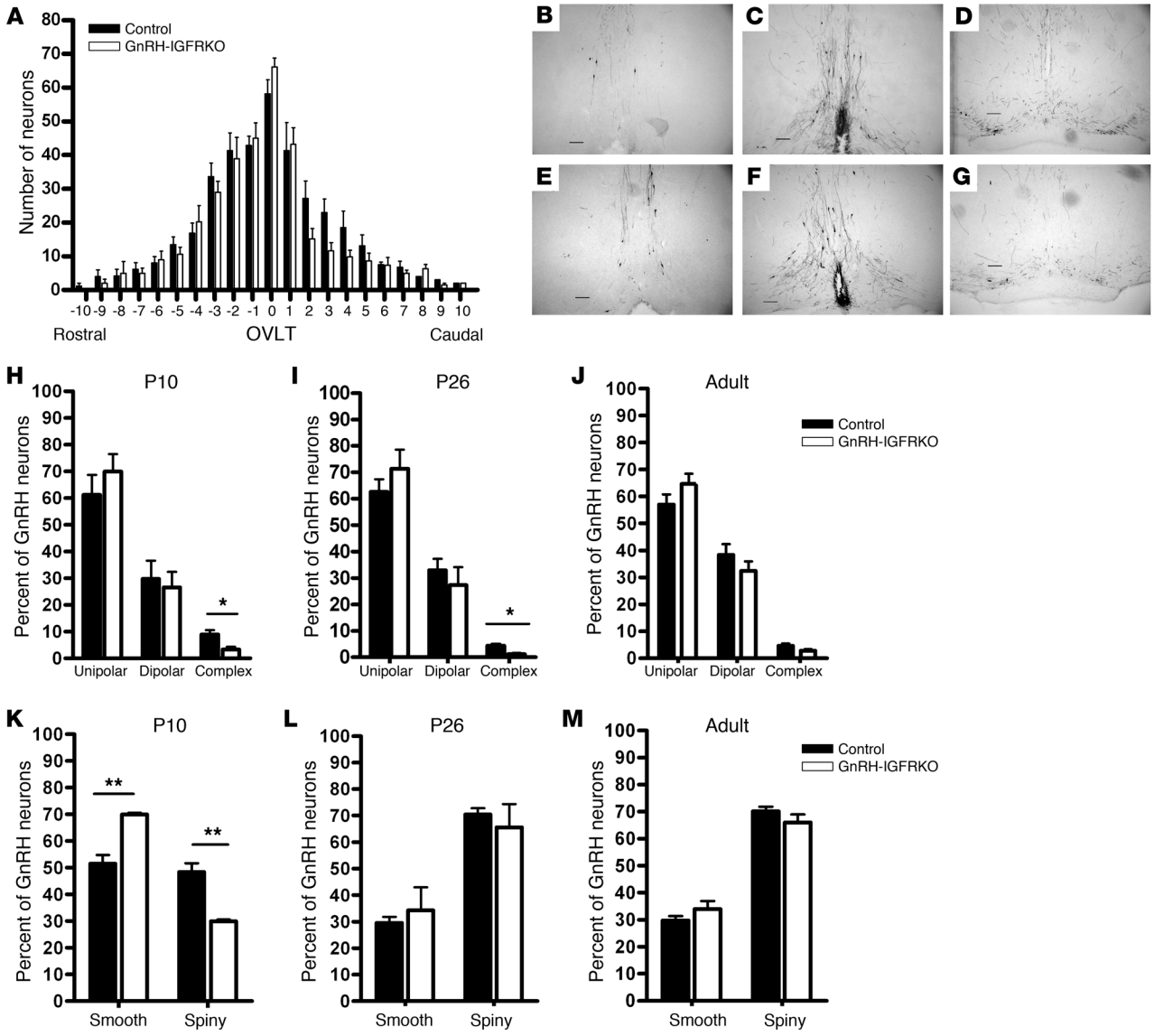

Figure 7

Developmental differences in GnRH neuronal morphology are present in GnRH-IGFRKO mice. Forty-micrometer sections of hypothalami from control mice or GnRH-IGFRKO were stained for GnRH immunoreactivity. (**A**) Graph of the number of GnRH neurons counted in control ($n = 6$) versus GnRH-IGFRKO ($n = 6$) adult mice. OVLT is labeled as 0. Each interval graphed encompasses 160 μm, thus 4 successive slices. Images (original magnification, ×100) show an area 640 mm rostral to OVLT (**B**), the OVLT (**C**), and an area 640 mm caudal to OVLT (**D**) in control and GnRH-IGFRKO (**E**–**G**) mice. Scale bars: 100 μm. Dendritic structure of individual GnRH neurons was determined in P10 (**H**), P26 (**I**), and adult (**J**) mice. $n = 3$ mice for each postnatal day and genotype. The irregularity of individual GnRH neurons was determined in P10 (**K**), P26 (**L**), and adult (**M**) mice. $n = 3$ mice of each postnatal day and genotype. Values are mean ± SEM. $^{*}P < 0.05$, $^{**}P < 0.01$.

in the number or distribution of GnRH neurons in control versus GnRH-IGFRKO mice. Figure 7, B–D, shows representative coronal sections in a P26 control littermate mouse that include a region 640 μm rostral to the organum vasculosum of the lamina terminalis (OVLT; –4 in Figure 7A), the OVLT (Figure 7C), and a region 640 μm caudal to the OVLT (Figure 7D; +4 in Figure 7A). Corresponding regions in a P26 GnRH-IGFRKO mouse are shown in Figure 7, E–G. No significant difference in neuron number or GnRH fibers was noted between control and GnRH-IGFRKO mice.

GnRH neurons undergo changes in neurite outgrowth during normal development. Most GnRH neurons have unipolar or dipolar dendritic processes, but some neurons have a complex dendritic structure, with 3 or more processes emanating from the cell body. The percentage of GnRH neurons that exhibit a complex dendritic structure decreases during postnatal development, reaching the low adult levels by puberty (28). Thus, we examined the dendritic morphology of GnRH neurons in prepubertal control and GnRH-IGFRKO mice on P10, in pubertal mice on P26, and in adult mice. On P10, the percentage of dipolar and unipolar neurons in GnRH-IGFRKO mice was similar to that in control mice (Figure 7H), while GnRH-IGFRKO mice had a significantly smaller percentage of cells with a complex configuration (con-

trol, 8.8% ± 1.7% vs. GnRH-IGFRKO, 3.3% ± 0.9%, $P < 0.05$; Figure 7H). On P26, GnRH-IGFRKO mice again exhibited a significantly smaller percentage of complex cells (control, 4.3% ± 0.7% vs. GnRH-IGFRKO, 1.4% ± 0.7%, $P < 0.05$; Figure 7I). However, the percentage of complex cells in adult GnRH-IGFRKO mice was similar to that in control mice (Figure 7J).

During development, GnRH neurons also undergo changes in the percentage of cells with spiny processes; the percentage of total neurons with spines is lowest at birth and increases gradually postnatally until puberty (29). Therefore we assessed whether neurons had a smooth contour with virtually no irregularities disrupting the outline of the cell or had spiny processes that rendered the neuron irregular. On P10, GnRH-IGFRKO mice had significantly higher percentage of smooth neurons (control, 51.3% ± 3.3% vs. GnRH-IGFRKO, 69.3% ± 0.6%, $P < 0.05$; Figure 7K) and a lower percentage of spiny neurons compared with control mice. P26 (Figure 7L) and adult (Figure 7M) GnRH-IGFRKO mice had similar numbers of smooth and spiny neurons compared with control mice.

Discussion

The hormonal, nutritional, and environmental status of the mammal must be optimal to allow the reawakening of the GnRH neuron at puberty. In this study, we have further defined the roles of the growth factors insulin and IGF-1 in the central control of reproduction, finding that IGF receptor, but not IR, signaling in the GnRH neuron is crucial for the normal timing of pubertal onset.

We show that IR signaling in the GnRH neuron is not crucial to the function of the GnRH neuron at puberty, as indicated by the normal timing of vaginal opening, first estrus, preputial separation, and AGD in GnRH-IRKO mice (Figure 2, A and B). In addition, female and male reproductive function in the healthy adult was also intact, as indicated by the normal fertility and LH levels in females and males (Figure 2, F and G) and estrous cycling in females (Figure 2, D and E). Thus, the female subfertility noted in NIRKO females may not be due to dysfunction directly at the level of the GnRH neuron. The loss of IRs in proopiomelanocortin- or agouti-related peptide–expressing (POMC- or AgRP-expressing) neurons — neurons involved in the regulation of appetite and peripheral metabolism of glucose and fat — also did not affect fertility (30). Thus, the neuronal location of IR regulation of reproduction, if present, is still not clear. The NIRKO mice exhibited obesity with associated metabolic derangements including insulin and leptin resistance and hypertriglyceridemia, raising the possibility that the infertility was secondary to the dysregulated hormonal milieu rather than the loss of IRs in neurons. In vitro, low concentrations of insulin that do not activate the IGF-1R have been shown to increase GnRH gene expression (14) in GnRH-secreting immortalized cell lines. Insulin also increases GnRH pulsatile secretion (16), suggesting that insulin pathways can be activated in the GnRH neuron. Although the dose of insulin used to achieve this effect may cause activation of the IGF-1R, IGF-1 infusion did not cause GnRH secretion in the protocol used. Alternatively, IR signaling in GnRH neurons, quiescent in normal conditions, may become activated in pathological states with a disrupted hormonal milieu such as obesity and lead to GnRH neuron dysfunction.

Serum IGF-1 levels increase at the time of puberty in rodents (31, 32), primates (33), and humans (34), suggesting that IGF-1 is a link between the somatotropic and gonadotropic axes at puberty. Studies investigating a causal role for IGF-1 in puberty have yielded mixed results. Systemic (9) and intracerebroventricular (7) IGF-1 administration has been shown to advance pubertal onset in rodents and accelerate puberty in primates (35). However, continuous IGF-1 administration via an osmotic pump to prepubertal rats did not significantly advance pubertal onset (36). Moreover, these studies did not address the locus of action of IGF-1. Daftary and Gore characterized the hypothalamic expression pattern of *Igf1* and *Igf1r* in developing rodents. Hypothalamic *Igf1* and *Igf1r* expression increases dramatically at the time of puberty and colocalize with GnRH neurons (13, 37). This temporal and spatial relationship implicates a role for GnRH neuronal IGF-1 signaling during puberty. To elucidate the role of IGF-1R in GnRH neurons, we generated mice with the absence of IGF-1R specifically in GnRH neurons (Figure 3). Both female and male mice experienced delayed puberty (Figures 4 and 5), providing direct evidence that IGF-1R signaling is necessary for the timely activation of GnRH neurons at puberty. The delayed pubertal onset was secondary to hypothalamic-pituitary dysfunction, as both female and male GnRH-IGFRKO mice had lower gonadotropin levels than control mice at an age when the control mice had entered puberty but the GnRH-IGFRKO mice had not (Figure 4C and Figure 5E). GnRH-IGFRKO mice eventually experienced pubertal onset, suggesting that IGF-1 pathway activation is not absolutely required for GnRH activation. Clearly, GnRH activation at puberty is dependent upon a spectrum of genetic, developmental, and environmental signals that must converge in a certain pattern. Loss of one signal, such as IGF-1R activation, may eventually be overcome by other environmental and/or developmental signals to induce GnRH pulse generator activity.

IGF-1R activation results in stimulation of pathways common to the IR. Indeed, at high concentrations, insulin can bind the IGF-1R and IGF-1 to the IR (38). The GnRH-specific IR-knockout mice of both sexes had normal pubertal timing and fertility (Figure 2). Although it is possible that IGF-1R activation compensates for the loss of IR activation in these mice, insulin levels in these mice were not significantly higher than in controls, so it is unlikely that the IGF-1R was activated by insulin. These data also indicate that the phenotype of delayed puberty observed in GnRH-IGFRKO mice is not due to neuron dysfunction from the presence of the Cre recombinase. It is possible that IR incompletely compensates for the lack of IGF-1R, accounting for the delayed but eventual activation of the GnRH pulse generator in the GnRH-IGFRKO mice. The development of a GnRH neuron IGF-1R/IR double-knockout mouse would be required to determine the extent of compensatory receptor upregulation.

Intracerebroventricular infusion of an IGF-1R antagonist to adult rats results in loss of estrous cyclicity not observed in rats administered vehicle (39). Estrous cyclicity is restored with coinfusion of IGF-1 and the receptor antagonist. Thus, hypothalamic IGF-1R signaling is implicated in rodent ovulation. In our studies, loss of IGF-1R in GnRH neurons did not affect adult reproductive function, as indicated by normal estrous cycling, fertility, and gonadotropin levels (Figures 4 and 5). This suggests that IGF-1R signaling neurons afferent to the GnRH neuron play a role in the regulation of estrous cycling.

Herbison et al. noted that mice with 12% of the normal GnRH neuronal population in the hypothalamus did not experience significantly delayed pubertal onset compared with wild-type mice, indicating that adequate GnRH pulsatility can be achieved by a small number of neurons (40). We observed that with a normal number of hypothalamic GnRH neurons (Figure 7, A–G), the GnRH-IGFRKO mice exhibited delayed puberty (Figures 4 and 5).

Together, these data indicate that the disordered pubertal timing in the GnRH-IGFRKO mouse is a result of GnRH neuron dysfunction, rather than inadequate GnRH neuron number.

Cre recombinase expression in the GnRH-Cre mouse used in this study begins at the time of GnRH expression, approximately day 11 after conception in the mouse (41). Thus, deletion of the *Igf1r* gene in the GnRH neuron likely occurs on day 11 after conception. At that time, GnRH neurons are present in the olfactory placode and migrate to the hypothalamus, reaching their final destination at day 17 after conception. The GnRH-IGFRKO mice had GnRH neuron distribution and number comparable to those in controls (Figure 7, A–G), implying that IGF-1R signaling pathways are not necessary for GnRH neuron migration.

IGF-1 signaling has been found to stimulate neurite outgrowth (27), and IGF-1–null mice exhibit a decrease in dendrite complexity in the cortex (42). The GnRH neuron population is composed of subpopulations of neurons with unipolar, dipolar, or complex dendritic trees (28). The greatest percentage of complex neurons is in prepubertal mice, with the percentage decreasing upon pubertal development, implying that dendritic remodeling occurs during normal development (28). We found that pre- and peripubertal GnRH-IGFRKO mice had a significantly smaller percentage of complex cells (Figure 7, H and I), while the percentages of unipolar and dipolar cells did not differ in the two groups at different developmental stages. These data suggest that IGF-1R signaling plays a role in the normal generation of the complex subtype of GnRH neurons and implicate complex dendritic structure, and the intricate communication with afferent neurons that the structure implies, in pubertal onset.

Several groups have shown that the percentage of GnRH neurons with an irregular surface (i.e., with spines) increases with postnatal development in rats, reaching a plateau after completion of puberty (28, 29). The spiny processes of neurons are the location of excitatory synapses important in neuronal plasticity (43), and IGF-1 signaling has been shown modulate neuronal spine density and size (44). When we examined the percentage of neurons with spines in prepubertal (P10), pubertal (P26), and adult control and GnRH-IGFRKO mice, we also noted a developmental increase in the proportion of spiny neurons (Figure 7, K–M). The GnRH-IGFRKO mice had a significantly lower proportion of neurons with spines at P10 but a similar proportion of spiny neurons at P26 and in adulthood. Thus, we postulate that IGF-1R signaling in the GnRH neuron facilitates the timely establishment of the synaptic structure necessary to receive afferent input. Together, these data indicate that IGF-1R plays a role in the prepubertal development of GnRH neuronal dendritic trees and synaptic structures that are important for receiving excitatory inputs for the induction of GnRH pulsation at pubertal onset.

IGF-1 peripherally administered to prepubertal mice significantly advanced puberty in control females but not in GnRH-IGFRKO females (Figure 6A). That the female GnRH-IGFRKO mice did not experience a significant advancement of pubertal onset unlike control littermates suggests that activation of IGF-1 signaling within the GnRH neuron is a primary trigger for increasing GnRH release at puberty. IGF-1 has recently been found to increase *Kiss1* gene expression in prepubertal female rats (45), and IGF-1 in the ovary synergizes with gonadotropins to stimulate steroid production and folliculogenesis of pre-ovulatory follicles (46). These pathways, intact in the GnRH-IGFRKO mouse, may account for the slight advancement of puberty with IGF-1 treatment observed in these animals. These pathways may also contribute to the advancement of puberty in control females receiving IGF-1. Supraphysiologic IGF-1 of peripheral origin advanced puberty; whether peripherally derived or centrally derived IGF-1 is responsible for the timely activation of the GnRH pulse generator in normal mice cannot be elucidated by these studies.

IGF-1 treatment of male mice did not affect puberty in control or GnRH-IGFRKO animals (Figure 6B). These data suggest that, unlike in females, activation of IGF signaling alone in GnRH neurons cannot activate the GnRH pulse generator; activation of IGF signaling pathways must be combined with activation or inhibition of other pathways to activate the GnRH pulse generator in males. Alternatively, males may need higher IGF-1 doses to effect pubertal onset. The sexual dimorphism of the effects of IGF-1 treatment on puberty is striking, although not surprising. IGF-1 has been shown to interact with estradiol to affect puberty. Primate studies have shown that IGF-1 treatment decreases the negative feedback effects of estrogen on LH release to advance the onset of puberty (47). Furthermore, the effect of intracerebroventricular IGF-1 treatment on rodent LH release is enhanced if detectable levels of serum estradiol are present (48). These effects are IGF-1R dependent (49). In addition, the timing of puberty in mammals is earlier in females than males, implying that activation of the GnRH pulse generator is under the control of additional and/or different signals, pathways, and mechanisms. Indeed, the differential effects of IGF-1 on male and female pubertal timing may partly account for the sexual dimorphism of pubertal timing seen in mammals.

Normal somatic and reproductive development can occur only in an anabolic state. The data presented here suggest that IGF-1 is an important anabolic factor that signals growth and metabolic status to the reproductive axis. Obesity is associated with earlier pubertal onset in female rodents (50) and girls (51) but not boys. In obesity, perturbations in the GH/IGF-1 system are observed, suggesting that IGF-1 is more bioavailable in obese children (52). We speculate that IGF-1 action directly on the GnRH neuron contributes to the trend of earlier pubertal onset uniquely seen in obese females.

In summary, IGF-1R signaling is necessary for timely activation of GnRH pulsation at puberty, and normal GnRH neuron dendritic tree and spiny process formation. Additionally, primary activation of receptor pathways by exogenous IGF-1 can hasten GnRH neuron activation and pubertal onset in females. These studies extend our understanding of the complex circuitry linking somatic development to reproductive function and provide insight into the sexual dimorphism of pubertal onset.

Methods

Animals. The GnRH-Cre mice developed in our laboratory (21) were maintained on a CD1 background. The IR floxed mice were maintained on a mixed CD1 and C57BL/6J background, while the IGF-1R floxed mice were maintained on a C57BL/6J background; thus, the GnRH-IRKO and GnRH-IGFRKO mice were a mixed CD1-C57BL/6J background. All experimental animals were from 4 founder matings each for GnRH-IRKO and GnRH-IGFRKO. At P21, the animals were housed in individual cages. Vaginal opening in females or balanopreputial separation in males was assessed daily. For determination of age of first estrus, vaginal cells were collected by saline lavage beginning the day of vaginal opening and continuing each day thereafter. If blood was obtained peripubertally via mandibular bleed after light sedation with isoflurane, the animal was subsequently sacrificed. Wet testicular weights were determined in freshly dissected animals. At 6 weeks, fertility studies were performed. To test female fertility, female mice were housed with a wild-type male mouse for 7 days, then separated.

Four females of each genotype were rotated between 2 wild-type males, and each female participated in at least 6 attempts at mating with at least 5 weeks between mating attempts. To test male fertility, males were housed continuously with 2 wild-type females and mating continued for 4 months.

For injectisons, P16 pups, housed with the dam, were assigned to receive vehicle or IGF-1 injections. There were 4 treatment groups: control mice receiving vehicle, control mice receiving IGF-1, GnRH-IGFRKO mice receiving vehicle, and GnRH-IGFRKO mice receiving IGF-1. IGF-1 (gift of Tercica Inc.) was dissolved in normal saline with 100 mM acetic acid and 1% bovine serum albumin. Mice were injected subcutaneously twice daily with vehicle or IGF-1 at a dose of 20 μg/g. This dose was empirically determined to cause earlier puberty in wild-type female mice. At P21, mice were individually housed, and IGF-1 or vehicle was continued until puberty was achieved.

All procedures were reviewed and approved by the Johns Hopkins University Animal Care and Use Committee.

Vaginal cytology. Vaginal cells were collected via saline rinse, dried, fixed with methanol, and then stained with Diff-Quick staining kit (IMEB Inc.). Estrous cycle staging was performed using the method of Nelson et al. (53). Briefly, proestrus was assigned when nucleated cells predominated; estrus was assigned when cornified cells predominated; metestrus when cornified cells and leukocytes were present; and diestrus when leukocytes predominated.

Perfusion and immunohistochemistry. Mice were deeply sedated with ketamine and xylazine, then the left ventricle was cannulated. After a normal saline rinse, mice were perfused transcardially with 4% paraformaldehyde. The brain was then removed, postfixed in 4% paraformaldehyde overnight, dehydrated in 30% sucrose for 24 hours, then frozen. Forty-micrometer sections were cut using a cryostat (Leica) beginning caudally in the septal-preoptic area and ending rostrally midway through the olfactory bulbs. For GnRH and IGF-1R double labeling, sections were rinsed with PBS, then blocked with 10% goat serum. Sections were then incubated for 96 hours with 1:500 mouse monoclonal GnRH antibody (gift of H. Urbanski, Oregon National Primate Research Center, Beaverton, Oregon, USA) and 1:500 rabbit IGF receptor antibody (Santa Cruz Biotechnology Inc.) in 2% goat serum. After rinsing in PBS, sections were incubated in anti-rabbit Alexa Fluor 488 (Invitrogen; 1:400) and anti-mouse Alexa Fluor 594 (1:400) for 1 hour. After rinsing with PBS, sections were mounted, then coated with VECTASHIELD (Vector Laboratories) and coverslipped. For the purpose of counting GnRH neurons, the sections were incubated in 0.5% hydrogen peroxide, rinsed with PBS, blocked in 2% goat serum, and then incubated overnight with rabbit anti-GnRH antibody (Affinity Bioreagents) at 1:10,000. Sections were rinsed and incubated in strepavidin-conjugated goat anti-rabbit secondary antibody (Vector Laboratories) for 1 hour. After another rinse, sections were then incubated in the ABC kit (Vector Laboratories) for 1 hour. After rinsing, sections were developed using DAB-nickel staining (Vector Laboratories), then mounted and dried overnight. Slides were dehydrated with ethanol, then coated with Permount and coverslipped. Sections were visualized using a Zeiss Axiovert microscope and the Axiovision version 4.6.3 imaging program. For analysis, results from male and female mice were combined, as the total number and morphology of neurons are similar between the sexes (29). Categorization of cells into the different dendritic morphologies was according to Cottrell et al. (28). Briefly, unipolar cells were defined as possessing a single process projecting from the cell body. Dipolar cells were defined as having 2 processes projecting from the cell body, and complex cells were defined as possessing 3 or more processes originating from the cell body or any branch point evident on proximal dendrites. Categorization of cells into a smooth or spiny configuration was according to Wray and Hoffman (29). Briefly, a cell was categorized as smooth if the cell soma and processes were smooth in contour, with virtually no irregularities disrupting the outline of the cell. Cells not meeting these criteria were classified as spiny.

Tissue extraction and PCR. After dissection and harvesting of tissue, genomic DNA was isolated using phenol-chloroform extraction and isopropanol precipitation. To determine presence of the Cre transgene, DNA was subjected to PCR using primers sense 5′-CGACCAAGTGACAGCAATGCT-3′ and antisense 5′-GGTGCTAACCAGCGTTTTCGT-3′. To identify for the presence of the IR floxed allele, the primers sense 5′-TGCACCCCATGTCTGGGACCC-3′ and antisense 5′-GCCTCCTGAATAGCTGAGACC-3′ were used. To identify tissues that had the IR truncated by Cre recombination, we used primers p1, p2, and p3 according to the strategy of Kulkarni et al. (54). To detect the presence of the IGF receptor floxed allele, the primers sense 5′-TCCCTCAGGCTTCATCCGCAA-3′ and antisense 5′-CTTCAGCTTTGCAGGTGCACG-3′ were used. To identify tissues that had the IGF-1R truncated by CRE recombination, the primers sense 5′-TTATGCCTCCTCTCTTCATC-3′ and antisense 5′-CTTCAGCTTTGCAGGTGCACG-3′ were used. To verify the presence of the intact *Igf1r* gene in various tissues, the sense primer 5′-ATGACCCAGGGGAGGCTGTGTA-3′ was used with the IGFR antisense primer.

Hormone assays. LH and FSH were analyzed by xMap technology (Millipore), using the rat pituitary panel. A standard curve was generated using 5-fold serial dilutions of the LH/FSH standard cocktail provided by the vendor. Standards and samples were incubated with the antibody-coated beads on a microplate shaker overnight at 4°C and washed 3 times using a vacuum manifold apparatus. Detection antibody was then added to the wells and incubated at room temperature for 30 minutes. Streptavidin-phycoerythrin solution was then added, followed by an additional 30-minute incubation at room temperature. Plates were then washed 3 times, and sheath fluid was added to each well. Beads were resuspended on the microplate shaker for 5 minutes. Plates were then read on the Luminex 200IS system with xPonent software (Luminex Corp.). Data were analyzed with 5-parameter logistic curve fitting. The limit of detection for the assay for LH was 48 pg/ml, and the intraassay coefficient of variance was between 6.3% and 9.0%. The limit of detection for the FSH assay was 96 pg/ml, and the intraassay coefficient of variance was between 2.8% and 6.7%. The interassay coefficient of variance was between 12.0% and 14.6% for standard LH and FSH low and high pools. Radioimmunoassays for LH were also performed at the Ligand Assay Core of Northwestern University. The intraassay and interassay coefficients of variance were less than 10%. Insulin was analyzed by xMAP technology, similar to LH and FSH analysis. The limit of detection of the insulin assay was 0.1 ng/ml, and the intraassay coefficient of variance was between 0.4% and 3.4%. The interassay coefficient of variance was between 18.1% and 6.5% for low and high pools, respectively.

Statistics. Data were graphed using the GraphPad Prism 4 program (GraphPad Software). Values are expressed as mean ± SEM. If data satisfied Bartlett tests for equal variances, parametric statistics such as Student's *t* test were used to determine significance of differences between control and GnRH-specific knockout mice. For analysis of neuron morphology, Mann-Whitney *U* test was used. Two-way ANOVA with Bonferroni post-test was used to evaluate weight, AGD, testicular weight, and response to IGF-1 administration. Significance was assigned if P was less than 0.05.

Acknowledgments

The authors thank Brigitte Mann of the Northwestern University Ligand Assay Core Facility for performing the LH radioimmunoassays. We also thank Andrea Gore for helpful advice regarding GnRH and IGF-1R immunofluorescence staining. This work was supported by the Lawson Wilkins Pediatric Endocrine Society (LWPES) Clinical Scholars Award and NIH K08HD056139 to S.A. DiVall, Deutsche Forschungsgemeinschaft (DFG) Br1492-7 to J.C. Brüning, NIH R01HD044608 to A. Wolfe, and the Eunice Kennedy Shriver NICHD/NIH through cooperative agreement

U54HD41859 as part of the Specialized Cooperative Centers Program in Reproduction and Infertility Research.

Received for publication September 4, 2009, and accepted in revised form May 26, 2010.

Address correspondence to: Sara A. DiVall, Division of Pediatric Endocrinology, Department of Pediatrics, Johns Hopkins University, 600 N. Wolfe Street, CMSC 406, Baltimore, Maryland 21212, USA. Phone: 410.502.7573; Fax: 410.502.7580; E-mail: sdivall1@jhmi.edu.

1. Palmert MR, Boepple PA. Variation in the timing of puberty: Clinical spectrum and genetic investigation. *J Clin Endocrinol Metab*. 2001;86(6):2364–2368.
2. Frisch RE, Revelle R. Height and weight at menarche and a hypothesis of critical body weights and adolescent events. *Science*. 1970;169(943):397–399.
3. Frisch RE, Hegsted DM, Yoshinaga K. Body weight and food intake at early estrus of rats on a high-fat diet. *Proc Natl Acad Sci U S A*. 1975;72(10):4172–4176.
4. Nathan BM, Palmert MR. Regulation and disorders of pubertal timing. *Endocrinol Metab Clin North Am*. 2005;34(3):617–641, ix.
5. Bruning JC, et al. Role of brain insulin receptor in control of body weight and reproduction. *Science*. 2000; 289(5487):2122–2125.
6. Savage M, et al. Clinical features and endocrine status in patients with growth hormone insensitivity (Laron syndrome). *J Clin Endocrinol Metab*. 1993; 77(6):1465–1471.
7. Hiney JK, Srivastava V, Nyberg CL, Ojeda SR, Dees WL. Insulin-like growth factor I of peripheral origin acts centrally to accelerate the initiation of female puberty. *Endocrinology*. 1996;137(9):3717–3728.
8. Pazos F, Sanchez-Franco F, Balsa J, Lopez-Fernandez J, Escalada J, Cacicedo L. Regulation of gonadal and somatotropic axis by chronic intraventricular infusion of insulin-like growth factor 1 antibody at the initiation of puberty in male rats. *Neuroendocrinology*. 1999;69(6):408–416.
9. Danilovich N, Wernsing D, Coschigano KT, Kopchick JJ, Bartke A. Deficits in female reproductive function in GH-R-KO mice; role of IGF-I. *Endocrinology*. 1999;140(6):2637–2640.
10. Keene DE, Suescun MO, Bostwick MG, Chandrashekar V, Bartke A, Kopchick JJ. Puberty is delayed in male growth hormone receptor gene–disrupted mice. *J Androl*. 2002;23(5):661–668.
11. Kim HH, DiVall SA, Deneau RM, Wolfe A. Insulin regulation of GnRH gene expression through MAP kinase signaling pathways. *Mol Cell Endocrinol*. 2005; 242(1–2):42–49.
12. Zhen S, Zakaria M, Wolfe A, Radovick S. Regulation of gonadotropin-releasing hormone (GnRH) gene expression by insulin-like growth factor i in a cultured GnRH-expressing neuronal cell line. *Mol Endocrinol*. 1997;11(8):1145–1155.
13. Daftary SS, Gore AC. The hypothalamic insulin-like growth factor-1 receptor and its relationship to gonadotropin-releasing hormones neurones during postnatal development. *J Neuroendocrinol*. 2004; 16(2):160–169.
14. DiVall SA, Radovick S, Wolfe A. Egr-1 binds the GnRH promoter to mediate the increase in gene expression by insulin. *Mol Cell Endocrinol*. 2007;270(1–2):64–72.
15. Salvi R, et al. Gonadotropin-releasing hormone-expressing neurons immortalized conditionally are activated by insulin: implication of the mitogen-activated protein kinase pathway. *Endocrinology*. 2006;147(2):816–826.
16. Burcelin R, Thorens B, Glauser M, Gaillard RC, Pralong FP. Gonadotropin-releasing hormone secretion from hypothalamic neurons: stimulation by insulin and potentiation by leptin. *Endocrinology*. 2003;144(10):4484–4491.
17. Zhen S, Zakaria M, Wolfe A, Radovick S. Regulation of gonadotropin-releasing hormone (GnRH) gene expression by insulin-like growth factor I in a cultured GnRH-expressing neuronal cell line. *Mol Endocrinol*. 1997;11(8):1145–1155.
18. Longo KM, Sun Y, Gore AC. Insulin-like growth factor-i effects on gonadotropin-releasing hormone biosynthesis in GT1-7 cells. *Endocrinology*. 1998; 139(3):1125–1132.
19. Anderson RA, Zwain IH, Arroyo A, Mellon PL, Yen SS. The insulin-like growth factor system in the GT1-7 GnRH neuronal cell line. *Neuroendocrinology*. 1999; 70(5):353–359.
20. Bruning JC, et al. A muscle-specific insulin receptor knockout exhibits features of the metabolic syndrome of NIDDM without altering glucose tolerance. *Mol Cell*. 1998;2(5):559–569.
21. Wolfe A, et al. Temporal and spatial regulation of CRE recombinase expression in gonadotrophin-releasing hormone neurones in the mouse. *J Neuroendocrinol*. 2008;20(7):909–916.
22. Safranski T, Lamberson W, Keisler D. Correlations among three measures of puberty in mice and relationships with estradiol concentration and ovulation. *Biol Reprod*. 1993;48(3):669–673.
23. Korenbrot CC, Huhtaniemi IT, Weiner RI. Preputial separation as an external sign of pubertal development in the male rat. *Biol Reprod*. 1977;17(2):298–303.
24. Lapatto R, et al. Kiss1–/– mice exhibit more variable hypogonadism than Gpr54–/– mice. *Endocrinology*. 2007;148(10):4927–4936.
25. Kloting N, et al. Autocrine IGF-1 action in adipocytes controls systemic IGF-1 concentrations and growth. *Diabetes*. 2008;57(8):2074–2082.
26. Stachelscheid H, et al. Epidermal insulin/IGF-1 signalling control interfollicular morphogenesis and proliferative potential through Rac activation. *EMBO J*. 2008;27(15):2091–2101.
27. Joseph D'Ercole A, Ye P. Expanding the mind: Insulin-like growth factor I and brain development. *Endocrinology*. 2008;149(12):5958–5962.
28. Cottrell EC, Campbell RE, Han S, Herbison AE. Postnatal remodeling of dendritic structure and spine density in gonadotropin-releasing hormone neurons. *Endocrinology*. 2006;147(8):3652–3661.
29. Wray S, Hoffman G. Postnatal morphological changes in rat LHRH neurons correlated with sexual maturation. *Neuroendocrinology*. 1986;43(2):93–97.
30. Konner AC, et al. Insulin action in AgRP-expressing neurons is required for suppression of hepatic glucose production. *Cell Metab*. 2007;5(6):438–449.
31. Handelsman DJ, Spaliviero JA, Scott CD, Baxter RC. Hormonal regulation of the peripubertal surge of insulin-like growth factor-i in the rat. *Endocrinology*. 1987;120(2):491–496.
32. Crawford BA, Singh J, Simpson JM, Handelsman DJ. Androgen regulation of circulating insulin-like growth factor-I during puberty in male hypogonadal mice. *J Endocrinol*. 1993;139(1):57–65.
33. Copeland KC, Kuehl TJ, Castracane VD. Pubertal endocrinology of the baboon: elevated somatomedin-C/insulin-like growth factor i at puberty. *J Clin Endocrinol Metab*. 1982;55(6):1198–1201.
34. Luna AM, et al. Somatomedins in adolescence: a cross-sectional study of the effect of puberty on plasma insulin-like growth factor I and II levels. *J Clin Endocrinol Metab*. 1983;57(2):268–271.
35. Wilson M. Premature elevation in serum insulin-like growth factor-I advances first ovulation in rhesus monkeys. *J Endocrinol*. 1998;158(2):247–257.
36. Gruaz NM, et al. Effects of constant infusion with insulin-like growth factor-I (IGF-I) to immature female rats on body weight gain, tissue growth and sexual function. Evidence that such treatment does not affect sexual maturation of fertility. *Endocrine*. 1997;6(1):11–19.
37. Daftary SS, Gore AC. Developmental changes in hypothalamic insulin-like growth factor-1: relationship to gonadotropin-releasing hormone neurons. *Endocrinology*. 2003;144(5):2034–2045.
38. Cheatham B, Kahn CR. Insulin action and the insulin signaling network. *Endocr Rev*. 1995;16(2):117–142.
39. Todd BJ, Fraley GS, Peck AC, Schwartz GJ, Etgen AM. Central insulin-like growth factor 1 receptors play distinct roles in the control of reproduction, food intake, and body weight in female rats. *Biol Reprod*. 2007;77(3):492–503.
40. Herbison AE, Porteous R, Pape J, Mora JM, Hurst PR. Gonadotropin-releasing hormone neuron requirements for puberty, ovulation, and fertility. *Endocrinology*. 2008;149(2):597–604.
41. Zheng L, Pfaff DW, Schwanzel-Fukuda M. Electron microscopic identification of luteinizing hormone-releasing hormone-immunoreactive neurons in the medial olfactory placode and basal forebrain of embryonic mice. *NeuroScience*. 1992;46(2):407–418.
42. Cheng CM, et al. Insulin-like growth factor 1 is essential for normal dendritic growth. *J Neurosci Res*. 2003;73(1):1–9.
43. Sorra KE, Harris KM. Overview on the structure, composition, function, development, and plasticity of hippocampal dendritic spines. *Hippocampus*. 2000;10(5):501–511.
44. Nieto-bona MP, Garcia-segura LM, Torres-alemán I. Transynaptic modulation by insulin-like growth factor I of dendritic spines in Purkinje cells. *Int J Dev Neurosci*. 1997;15(6):749–754.
45. Hiney JK, Srivastava VK, Pine MD, Dees WL. Insulin-like growth factor-I activates KiSS-1 gene expression in the brain of the prepubertal female rat. *Endocrinology*. 2009;150(1):376–384.
46. Kwintkiewicz J, Giudice LC. The interplay of insulin-like growth factors, gonadotropins, and endocrine disruptors in ovarian follicular development and function. *Semin Reprod Med*. 2009;27(1):43–51.
47. Wilson ME. IGF-I administration advances the decrease in hypersensitivity to oestradiol negative feedback inhibition of serum LH in adolescent female rhesus monkeys. *J Endocrinol*. 1995;145(1):121–130.
48. Hiney JK, Srivastava V, Dearth RK, Dees WL. Influence of estradiol on insulin-like growth factor-1-induced luteinizing hormone secretion. *Brain Res*. 2004;1013(1):91–97.
49. Quesada A, Etgen AM. Functional interactions between estrogen and insulin-like growth factor-I in the regulation of alpha 1B-adrenoceptors and female reproductive function. *J Neurosci*. 2002; 22(6):2401–2408.
50. Kirtley D, Maher R. Effect of an isocaloric high fat diet on initiation of puberty in osborne-mendel rats. *Biol Reprod*. 1979;21(2):331–338.
51. Euling SY, et al. Examination of US puberty-timing data from 1940 to 1994 for secular trends: panel findings. *Pediatrics*. 2008;121(suppl 3):S172–S191.
52. Ballerini MG, Ropelato MG, Domene HM, Pennisi P, Heinrich JJ, Jasper HG. Differential impact of simple childhood obesity on the components of the growth hormone-insulin-like growth factor (IGF)-IGF binding proteins axis. *J Pediatr Endocrinol Metab*. 2004;17(5):749–757.
53. Nelson JF, Felicio LS, Randall PK, Sims C, Finch CE. A longitudinal study of estrous cyclicity in aging C57BL/6J mice: I. Cycle frequency, length and vaginal cytology. *Biol Reprod*. 1982;27(2):327–339.
54. Kulkarni RN, Bruning JC, Winnay JN, Postic C, Magnuson MA, Kahn CR. Tissue-specific knockout of the insulin receptor in pancreatic beta cells creates an insulin secretory defect similar to that in type 2 diabetes. *Cell*. 1999;96(3):329–339.